

Three-lane and multi-lane signatures of planets in planetesimal disks

Tatiana V. Demidova,^{1*} Ivan I. Shevchenko^{1,2}

¹*Pulkovo Observatory of the Russian Academy of Sciences, Pulkovskoye Avenue 65, St. Petersburg 196140, Russia*

²*Lebedev Physical Institute of the Russian Academy of Sciences, 53 Leninskiy Prospekt, Moscow 119991, Russia*

Accepted XXX. Received YYY; in original form ZZZ

ABSTRACT

In massive numerical experiments we show that a planet embedded in a planetesimal disk induces a characteristic multi-lane “planetosignature” representing a pattern of several stellar-centric rings. If the planet’s mass is large enough, the multi-lane signature degenerates to a three-lane one: then it consists of three rings, one bright coorbital with the planet, and two dark gaps in the radial distribution of the particles. The gaps correspond to orbital resonances 2:1 and 1:2 with the planet. This theoretical prediction may explain recent ALMA observations of the disk of HL Tau.

Key words: methods: numerical – protoplanetary disks – planet-disk interactions – binaries: general – stars: individual: HL Tau.

1 INTRODUCTION

The motion of massive bodies inside a planetesimal disk may produce structures stable on secular time scales. In a previous study [Demidova & Shevchenko \(2015\)](#), we explored how a secular single-arm spiral pattern emerged in a circumbinary planetesimal disk devoid of planets. Here we explore models with a planet embedded in a circumbinary disk; namely, we investigate the formation of patterns in such a disk, and compare the emerging patterns with those arising in the case when the central star is single.

2 MODEL

We model disks for two cases of the mass ratio of the central stellar binary: a circular binary with masses $m_1 = M_\odot$ and $m_2 = 0.2M_\odot$ (model 1) and a circular binary with masses $m_1 = m_2 = M_\odot$ (model 2). For comparison, we take the model of a single central star with mass $m = 1.2M_\odot$ (model 3). The orbital periods of the binaries in models 1 and 2 are both set to $P_b = 0.2$ yr. The planet of Jovian mass is put initially in a circular orbit around the stellar barycenter. Its orbital radius corresponds to mean motion resonances with the binary, the ratios of the orbital periods of the planet and the binary set equal to 5 : 1, 11 : 2, 6 : 1, 13 : 2, 7 : 1, 15 : 2, 8 : 1. The choice of this grid of locations is motivated by the existing data that the *Kepler* circumbinary planets are mostly located in resonance cells at the outer border of the chaotic region around the central binary (see [Popova & Shevchenko](#)

[2013, 2016](#); in particular, Table 3 in [Popova & Shevchenko 2016](#)). In model 3 (the host star is single), the planet’s orbit is started at the same grid of radial distances as in model 1. The disk consists of 20000 massless (passively gravitating) planetesimals initially distributed from 0.3 to 5.3 AU in the radial distance from the barycenter in such a way that the surface density Σ decreases with the radial distance r according to the law $\Sigma \propto r^{-1}$. In each model, the motion was computed for $5 \cdot 10^4$ yr.

3 PATTERNS

The performed simulations make evident an emerging ring-shaped pattern (consisting of the planetesimals in the “tadpole” and “horse-shoe” orbits), coorbital with the planet (see [Fig. 1](#), where the case of planetary resonance 8:1 with the central binary is illustrated). They are most pronounced in models 1 and 2. For a single host star (as in model 3), similar coorbital patterns were revealed in [Ozernoy et al. \(2000\)](#); [Quillen & Thorndike \(2002\)](#); [Kuchner & Holman \(2003\)](#).

To estimate the pattern appearance quantitatively, we calculate the surface density distribution along the radius from the barycenter: the planetesimal disk is subdivided into 320 annular bands with the radial step 0.02 AU, then the number of particles in each band is calculated and divided by the band area (thus, the local surface density is calculated as a function of the radial distance).

As revealed by [Wisdom \(1980\)](#), a chaotic band around the orbit of a small-mass body (planet) moving around a main body (star) exists, due to the overlap of first-order mean motion resonances $(p + 1) : p$ with the planet on the

* E-mail: proxima1@list.ru

inner side of the planet’s orbit, and resonances $p : (p + 1)$ on the outer side of the orbit (integer numbers $p \gg 1$). If $\mu \equiv m_2/(m_1 + m_2) \ll 1$ (where m_1 and m_2 are the masses of the planet and the star, respectively), in the planar circular restricted three-body problem the radial half-width of this band is given by

$$\Delta a_{\text{Wisdom}} \approx 1.3\mu^{2/7} a_p \quad (1)$$

(Duncan et al. 1989), where a_p is the semimajor axis of the planet’s orbit, or

$$\Delta a_{\text{Wisdom}} \approx 1.57\mu^{2/7} a_p \quad (2)$$

(Murray & Dermott 1999). Further on, we use the latter formula, because its validity was verified in Murray & Dermott (1999) in massive model simulations.

On the other hand, the radial half-width of the coorbital (with the planet) band of stable horse-shoe and tadpole orbits can be estimated as approximately equal to the radius of the Hill sphere (for an illustration see figure 3.28 in Murray & Dermott 1999). In the planar circular restricted three-body problem the Hill radius is given by

$$\Delta a_{\text{Hill}} \approx \left(\frac{\mu}{3}\right)^{1/3} a_p \approx 0.693\mu^{1/3} a_p \quad (3)$$

(see, e.g., Murray & Dermott 1999).

From equations (2) and (3) one has

$$\frac{\Delta a_{\text{Wisdom}}}{\Delta a_{\text{Hill}}} \approx 2.26\mu^{-1/21}. \quad (4)$$

Therefore, the ratio $\Delta a_{\text{Wisdom}}/\Delta a_{\text{Hill}}$ is very insensitive to the mass parameter: in the range of μ from 0.0005 (model 2) to 0.01 it is ≈ 3 , changing only slightly, from 3.25 to 2.81. (In model 1, where $\mu \approx 0.0008$, one has $\Delta a_{\text{Wisdom}}/\Delta a_{\text{Hill}} \approx 3.17$.) Therefore, in this broad range of μ , the radial extent of the material kept coorbital with the planet is expected to be about one third of the radial extent of the theoretical Wisdom gap. In other words, the central one third (in radial extent) of the Wisdom gap may contain stable horse-shoe and tadpole material.

Therefore, from the theoretical viewpoint, one may expect existence of a ring-like pattern, surrounding the orbit of the planet embedded in the planetesimal disk. This pattern consists of at least three lanes: the bright central one (which we designate further on as Bc, i.e., bright central, or bright coorbital), and two components of the broader Wisdom gap (which we designate further on as Dc^{int} and Dc^{ext}, i.e., dark central, or dark coorbital, internal and external). These two components arise due to the division of the theoretical Wisdom gap by the Bc lane.

As follows from Fig. 2, where the results of simulations in model 1 are presented, this three-lane complex is present in all panels. In each panel, the disk density profile has a strong peak at resonance 1:1 with the planet (this peak corresponds to the Bc lane), as well as prominent gaps corresponding to the Dc^{int} and Dc^{ext} lanes. This *planetosignature* is observed for all choices of the initial radial location of the planet.

What is more, in each panel one observes additional

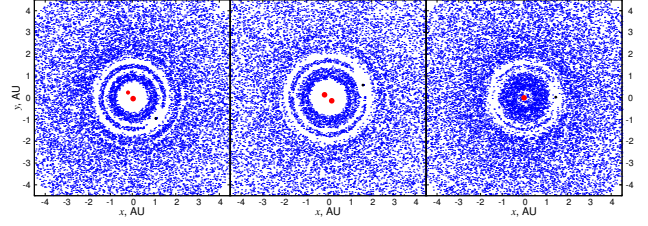


Figure 1. The evolved distributions of planetesimals in models 1, 2, and 3 (from left to right).

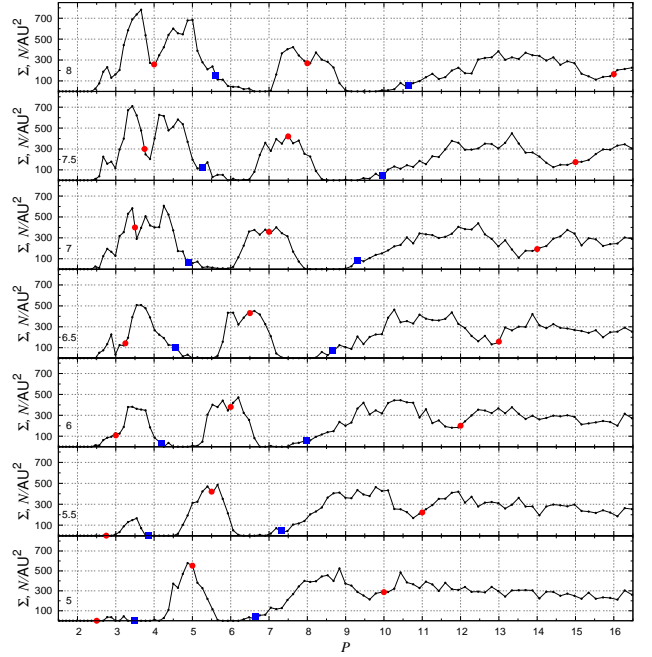


Figure 2. The local surface density as a function of the planet’s orbital period (in units of the host binary’s period) in model 1. Resonance of the planet with the host binary is specified at the left bottom corner of each panel. The red dots indicate the location of mean motion resonances 2:1, 1:1, 1:2 of planetesimals with the planet. The blue squares indicate the location of the Wisdom gap borders, according to formula (2).

pronounced minima, which are located at mean motion resonances 2:1 and 1:2 with the planet. We designate the corresponding lanes as D_{2:1} and D_{1:2} (the dark lanes at resonances 2:1 and 1:2). They are separated from the central three-lane complex Dc^{int}–Bc–Dc^{ext} by two (internal and external) bright lanes, which we designate as Bb^{int} and Bb^{ext} (“bright barriers”).

In total, one has a multi-lane (in fact, seven-lane) complex: D_{2:1}–Bb^{int}–Dc^{int}–Bc–Dc^{ext}–Bb^{ext}–D_{1:2}.

In models 2 and 3 (Fig. 3), the central three-lane complex appears to be basically the same. However, the D_{2:1} and D_{1:2} lanes are prominent only in the models with large enough planetary orbits. Therefore, depending on the system parameters, the observed pattern can be either three-lane or seven-lane. The three-lane pattern can arise, instead of the generic seven-lane pattern, in two cases: (1) simply

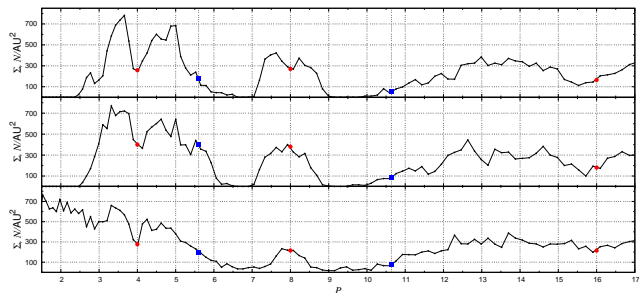


Figure 3. The local surface density as a function of the planet’s orbital period (in units of the host binary’s period) in models 1, 2 and 3 (from top to bottom). The first two panels correspond to the case of resonance 8:1 of the planet with the host binary. The red dots indicate the location of mean motion resonances 2:1, 1:1, 1:2 of planetesimals with the planet. The blue squares indicate the location of the Wisdom gap borders, according to formula (2).

because the 2:1 and 1:2 resonances are not prominent, (2) if the $D_{2:1}$ and $D_{1:2}$ lanes overlap, respectively, with the Dc^{int} and Dc^{ext} lanes (thus, the “bright barriers” Bb vanish). In the second case, the basic minima in the particle distribution shift to resonances 2:1 and 1:2 (whereas the Bc lane broadens); therefore, the observable pattern can be designated as $D_{2:1}\text{--}Bc\text{--}D_{1:2}$.

Let us derive an approximate condition for the second case. This can be done by equating the Wisdom gap borders’ locations (given by equation (2)) to the locations of resonances 2:1 and 1:2 (given by Kepler’s third law). One has two equations, for the inner and outer borders: $1 - 1.57\mu^{2/7} = 2^{-2/3} \approx 0.63$ and $1 + 1.57\mu^{2/7} = 2^{2/3} \approx 1.59$. Solving them, one has two approximate critical values of μ : 0.006 and 0.03, respectively. They are very approximate, as Wisdom’s theory is suitable at small values of μ only (see figure 2 in Shevchenko 2015). Therefore, we adopt the critical μ value ~ 0.01 . At such values of μ one expects the degeneration of the seven-lane complex into the three-lane one.

For a single host star, rather pronounced gaps at resonance 2:1 and at resonance 1:2 (in separate models) with the planet of 5 Jovian masses were found recently in Tabeshian & Wiegert (2016). The gaps originated on the time scale of 10^5 yr. Here we find that the opening of the resonant gaps $D_{2:1}$ and $D_{1:2}$ is much more pronounced in circumbinary disks than in a disk of a single host star.

The reason seems to be as follows: the presence of a stellar companion induces more secondary resonances in the neighborhood of both resonances 2:1 and 1:2, and their overlap causes more chaos in the phase space of motion. However note that, on the other hand, the stellar companion presence also induces precession of the planetary and planetesimal orbits, and in case of fast differential precession the splitting of resonances might be great enough to prevent the overlap; for an analysis of similar situations see El Moutamid et al. (2014).

The emergence of resonant gaps $D_{2:1}$ and $D_{1:2}$ themselves is theoretically expectable, as both resonances 2:1 and 1:2 may induce large zones of instability in the phase space

Table 1. The ratio of final and initial populations of the coorbital ring

P_p/P_b	5	5.5	6	6.5	7	7.5	8
Model 1	0.907	0.916	0.949	0.947	0.906	0.942	0.942
Model 2	0.916	0.932	0.928	0.928	0.931	0.908	0.920
Model 3	0.585	0.521	0.494	0.468	0.388	0.433	0.448

Note: The initial and final populations correspond to time $t = 1000$ yr and $t = 50000$ yr, respectively.

of motion, depending on initial conditions and system parameters (see Morbidelli 2002).

The circumbinary central cavities evident in the density profiles and in the snapshots of the evolved circumbinary disks are a natural outcome of the disk evolution, because a large central chaotic circumbinary zone exists at all eccentricities of the planetesimal if $\mu \gtrsim 0.05$ (Shevchenko 2015), where $\mu = m_2/(m_1 + m_2)$ is the mass parameter of the binary. According to empirical criteria derived by Holman & Wiegert (1999), the expected radii of the central chaotic zone should be $\approx 2.2a_b$ and $\approx 2.4a_b$ in models 1 and 2, respectively. This agrees well with the results of our simulations: the innermost maxima of the particle distributions in Figs. 2 and 3 are situated basically at $a/a_b \approx 2.3$ ($a/a_b = (P/P_b)^{2/3}$, where $P/P_b \approx 3.5$).

In the density profiles, the 1:1 peak corresponds to the ring-like pattern coorbital with the planet (i.e., the Bc lane). To characterize the “survivability” of the Bc lane, we compute the surface density Σ (averaged over the ring) as a function of time, in all three models. The radial boundaries of the Bc lane in models 1 and 2 are set at the radii where the local surface density Σ goes to zero, and the boundaries in model 3 are chosen to be the same as in model 1. The surface density Σ is defined as the number of particles moving inside the ring boundaries, divided by the ring area.

The problem on the stability of planetesimal motion in protoplanetary disks of multiple stars was discussed earlier in Verrier & Evans (2006, 2007, 2008). Here we find that the survivability of the coorbital ring pattern turns out to be rather different in disks of binary and single host stars: unexpectedly enough, it seems to be much greater in the binary case. This is illustrated in Table 3: in model 3, the percentage of surviving particles is ~ 2 times less than in the first two models.

4 APPLICATION TO THE HL TAU DISK

Planet-like “clumps” and coorbital and neighbouring ring-like patterns are directly observed now in circumstellar disks (Carrasco-González et al. 2016). Our inference that a multi-lane pattern can be generated by a planet embedded in a planetesimal disk may explain recent ALMA observations of the disk of HL Tau.

As follows from figure 3 in Carrasco-González et al. (2016), dark ring-like features D1 and D2 are situated at relative radii ≈ 0.63 and ≈ 1.60 (if the radius of the main bright feature B1, that with a planet-like “clump”, is set to unity). These numbers practically coincide with $2^{-2/3} \approx 0.63$

and $2^{2/3} \approx 1.59$, corresponding to mean motion resonances 2:1 and 1:2 with the clump. Therefore, they correspond to the D_{2:1} and D_{1:2} lanes in our models. Why the pattern here is three-lane, not the generic seven-lane?

Arguing that the emission from the clump is dominated by thermal dust emission, Carrasco-González et al. (2016) estimate a dust mass in the clump in the range 3–8 Earth masses. Setting the dust-to-gas ratio equal to the standard value 1/100, one obtains 1–3 Jovian masses for the full mass of the clump. On the other hand, the mass of the HL Tau star is $\approx 0.55M_{\odot}$ (Beckwith et al. 1990). Therefore, the mass parameter of the star-clump system can be estimated as $\mu \sim 0.002\text{--}0.006$. As discussed in the previous Section, the D_{2:1}–Bc–D_{1:2} three-lane pattern is expected to emerge at $\mu \gtrsim 0.01$. Taking into account that the both estimates are approximate, we conclude that the D_{2:1}–Bc–D_{1:2} interpretation of the observed pattern is rather plausible.

Let us note that other interpretations of the HL Tau disk structure may exist. Tamayo et al. (2015) introduced multiple-planet models with two inner planets located in the D1 and D2 gaps in the HL Tau disk, thus explaining the opening of the gaps by the purging effect of the planets.

When applying our model inferences to HL Tau, it is important to note that the single-star case corresponds to our model 3. In the bottom panel of Fig. 3 we see that the 2:1 and 1:2 patterns are less pronounced in model 3 than in models 1 and 2 (corresponding to the circumbinary case and represented in the upper panels). On the other hand, the mass parameter adopted in all our models is rather low ($\mu \sim 0.001$); and, as noted above, according to simulations by Tabeshian & Wiegert (2016) for a planet of 5 Jovian masses (i.e., 5 times greater than in our model 3) orbiting around a single star, the 2:1 and 1:2 gaps generated in the disk are rather pronounced.

It is also important to point out that our model disks are planetesimal, whereas the HL Tau disk is gas-dust. The presence of gas may affect the process of forming the disk patterns. The dust experiences aerodynamic drag, and the disk’s viscosity refills the opening gaps (Goldreich & Tremaine 1980). The formation of gaps can be retarded or they may be smoothed. In future it would be important to consider how the dissipation effects may alter the presented picture.

In this connection we note that there exist various estimates of the HL Tau system age: from ~ 0.2 Myr (Guilloteau et al. 2011) to ~ 1 Myr (Beckwith et al. 1990); and this is 4–20 greater than our typical simulation time (0.05 Myr). However, it should be taken into account that the mass of HL Tau is 2.2 times less than the stellar mass in our model 3. This means that the timescales measured in planetary periods are 1.5 times less different: they are in the range 2.7–13. According to Table 1, the Bc lane in the single star model is depleted rather quickly; therefore, our model 3 result may favour low values for the HL Tau system age. To judge whether this is the case, future integrations on longer timescales are required, as well as taking the gas presence into account.

5 CONCLUSIONS

We conclude that any observed presence of ring-like patterns in circumbinary disks may betray the existence of a planet that “shepherds” the ring. What is more, the planet’s mass can be estimated by measuring the radial extents of the pattern components.

Our model simulations show that a planet embedded in a planetesimal disk may induce a characteristic multi-lane “planetosignature” — a pattern consisting of several stellar-centric rings. The planetary multi-lane pattern seems to reveal itself most definitely in circumbinary disks.

If the planet’s mass is large enough ($\mu \gtrsim 0.01$), the multi-lane signature degenerates to a three-lane one: then it consists of three rings, one bright coorbital with the planet, and two dark gaps in the radial distribution of the particles. The gaps correspond to orbital resonances 2:1 and 1:2 with the planet. This theoretical prediction may explain recent ALMA observations of the disk of HL Tau.

Finally, we note that the currently used general definition of a planet (in the definition’s part requiring the planet to purge a neighborhood of its orbit IAU 2006) may need a reformulation, if one wishes the circumbinary planets to be encompassed by this definition, because the survivability of the coorbital planetesimal ring seems to be outstanding for such planets.

ACKNOWLEDGEMENTS

It is a pleasure to thank the referee for most valuable and useful remarks. This work was supported in part by the Russian Foundation for Basic Research (projects Nos. 14-02-00319 and 14-02-00464) and the Programmes of Fundamental Research of the Russian Academy of Sciences “Fundamental Problems of Nonlinear Dynamics” and “Fundamental Problems of the Solar System Study and Exploration”. The computations were partially carried out at the St. Petersburg Branch of the Joint Supercomputer Centre of the Russian Academy of Sciences.

REFERENCES

- Beckwith S. V. W., Sargent A. I., Chini R. S., Guesten R., 1990, *AJ*, **99**, 924
 Carrasco-González C., et al., 2016, *ApJ*, **821**, L16
 Demidova T. V., Shevchenko I. I., 2015, *ApJ*, **805**, 38
 Duncan M., Quinn T., Tremaine S., 1989, *Icarus*, **82**, 402
 El Moutamid M., Sicardy B., Renner S., 2014, *Celestial Mechanics and Dynamical Astronomy*, **118**, 235
 Goldreich P., Tremaine S., 1980, *ApJ*, **241**, 425
 Guilloteau S., Dutrey A., Piétu V., Boehler Y., 2011, *A&A*, **529**, A105
 Holman M. J., Wiegert P. A., 1999, *AJ*, **117**, 621
 IAU 2006, General Assembly:Result of the IAU Resolution votes.
 Kuchner M. J., Holman M. J., 2003, *ApJ*, **588**, 1110
 Morbidelli A., 2002, *Modern celestial mechanics : aspects of solar system dynamics*. London; New York : Taylor & Francis
 Murray C. D., Dermott S. F., 1999, *Solar system dynamics*. Cambridge; New York : Cambridge University Press
 Ozeronoy L. M., Gorkavyy N. N., Mather J. C., Taidakova T. A., 2000, *ApJ*, **537**, L147
 Popova E. A., Shevchenko I. I., 2013, *ApJ*, **769**, 152
 Popova E. A., Shevchenko I. I., 2016, *Astronomy Letters*, **42**, 260

- Quillen A. C., Thorndike S., 2002, [ApJ](#), **578**, L149
Shevchenko I. I., 2015, [ApJ](#), **799**, 8
Tabeshian M., Wiegert P. A., 2016, [ApJ](#), **818**, 159
Tamayo D., Triaud A. H. M. J., Menou K., Rein H., 2015, [ApJ](#),
805, 100
Verrier P. E., Evans N. W., 2006, [MNRAS](#), **368**, 1599
Verrier P. E., Evans N. W., 2007, [MNRAS](#), **382**, 1432
Verrier P. E., Evans N. W., 2008, [MNRAS](#), **390**, 1377
Wisdom J., 1980, [AJ](#), **85**, 1122